Available online at http://www.journalcra.com

International Journal of Current Research
Vol. 7, Issue, 10, pp.21709-21719, October, 2015

INTERNATIONAL JOURNAL OF CURRENT RESEARCH

ISSN: 0975-833X

RESEARCH ARTICLE

AIR COOLING OF ELECTRONIC COMPONENTS IN PARTIALLY TOP VENTED ENCLOSURES

***,[1]Sarhan, H. H., [2]Elbakhshawangy H. F. and [2]Abd El-Kawi O. S.**

[1]Mechanical Power Engineering Dept., Faculty of Engineering, Port Said University, Egypt
[2]Reactors Dept., Atomic Energy Authority of Egypt, P.O. Box: 13759, Cairo, Egypt

ARTICLE INFO

Article History:
Received 16th July, 2015
Received in revised form
20th August, 2015
Accepted 17th September, 2015
Published online 31st October, 2015

Key words:

Cooling of electronic components,
Vented enclosure,
Discrete heat source.

ABSTRACT

A three-dimensional study of steady laminar natural convection in partially top vented enclosure is investigated numerically. A discrete heat source mounted on the substrate at the bottom wall is used to simulate an electronic component. Three types of heat source are used with vent aspect ratio ranging from 0.0 to 0.1. The problem is described by continuity, momentum and energy partial differential equations, which are expressed in Cartesian coordinates system. The proposed governing equations are transformed to a set of dimensionless partial differential equations which, is solved with finite difference technique. A computer program is developed to solve the present proposed mathematical model. Solutions are obtained for Rayleigh number ranging from 1.0×10^4 to 1.0×10^6, enclosure aspect ratios ranging from 0.1 to 1.0 and Prandtl number 0f 0.7. The resulting flow and temperature patterns are discussed. Accordingly, the values of Nusselt number for different values of problem parameters are obtained. Comparisons between the present obtained results and the previous theoretical studies are performed for different values of problem parameters.

Nomenclature:

A	Area, m^2	x, y, z	Cartesian coordinates, m
AR	Aspect ratio L_3/L_1	X, Y, Z	Dimensionless Cartesian coordinates
C_p	Specific heat at constant pressure, J. kg^{-1}. K^{-1}	VAR	Vent aspect ratio, d_1/L_1
h	Local heat transfer coefficient, $W.m^{-2}$. K^{-1}	***Greek symbols***	
H	Volumetric Heat source, W. m^{-3}	μ	Dynamic viscosity, $kg.m^{-1}.s^{-1}$
k	Thermal conductivity of the fluid, $W.m^{-1}$. K^{-1}	ρ	Density, $kg.m^{-3}$
L	Length, m	α	Thermal diffusivity $(k/\rho C_p)$, $m^2.s^{-1}$
Nu_L	Local Nusselt number	ν	Kinematic viscosity, $m^2.s^{-1}$
Nu_{av}	Average Nusselt number	θ	Dimensionless temperature
p	Pressure, Pa	***Subscripts***	
P	Dimensionless pressure	*1*	Length in X - direction
Pr	Prandtl number	*2*	Length in Y - direction
q''	Heat flux, $W.m^{-2}$	*3*	Length in Z – direction
Ra	Rayleigh number	*w23*	Y- and Z-direction
s	Square vent side length, m		
T	Temperature, K	*w13*	X- and Z-direction
u, v, w	Velocity components in x,y,z coordinates, $m.s^{-1}$	*max*	Maximum
U, V, W	Dimensionless velocity components		

Citation: Sarhan, H. H., Elbakhshawangy H. F. and Abd El-Kawi O. S. 2015. "Air cooling of electronic components in partially top vented enclosures", *International Journal of Current Research*, 7, (10), 21709-21719.

INTRODUCTION

The study of natural convection inside vented enclosures with heat sources have received considerable attention because of their wide applications in thermal design of buildings, solar energy receivers with open enclosures, fire propagation in rooms and cooling of electronic devices. In many electronic components cooling situations, arrays of heat-dissipating components were mounted on vertical (or inclined) parallel plate channels that were opened to the ambient at opposite ends. The cooling of electronic components was one of the main barriers to developing faster, smaller, and more reliable systems. Moreover, the mass and energy transfer through openings in buildings by natural ventilation is found to have a significant impact on the indoor air quality. Also, in the case of fire scenario, the flow of air and combustion products across vents was governed the growth and spread of fires in buildings (Reay *et al*., 2013; Öztop *et al*., 2015).

****Corresponding author: Sarhan, H. H.***
Mechanical Power Engineering Dept., Faculty of Engineering, Port Said University, Egypt.

Firstly, the effects of different locations of active walls (hot and cold) on the thermal aspects were investigated in enclosures. The existing works available in literatures (Chadwick *et al*., 1991; Ho and Chang, 1994; Tou *et al*., 1999; Tou and Zhang 2003; Deng *et al*., 2002; Nithyadevi *et al*., 2007; Corcione and Habib, 2010; Rahman *et al*., 2013; Mahapatra *et al*., 2015) were related to shallow; square or tall differentially heated enclosures with partial heating and cooling, mainly emphasized in analyzing heat transfer and fluid-flow pattern in terms of Nusselt number and stream function.

Natural convection in a discretely heated enclosure was investigated experimentally and theoretically for single and multiple heater configurations (Chadwick *et al*., 1991). It was revealed that for the single heat source configuration, heater locations closer to the bottom of the enclosure yielded the highest heat transfer in the high Grashof number range. Discrete heat sources located near the enclosure bottom were, also, found to yield the highest heat transfer in the dual heater configuration.

Natural convection heat transfer inside a vertical rectangular enclosure with four two-dimensional discrete flush-mounted heaters was investigated numerically and experimentally to unveil, primarily, the influence of aspect ratio of the enclosure (Ho and Chang, 1994). Numerical simulation was conducted for aspect ratio varying from 1 to 10 with a given relative heater size and location. It was revealed that, the increase of the aspect ratio lead to substantial degradation of convective dissipation from the discrete heaters.

A three-dimensional numerical model was developed to investigate the effects of inclination on the heat transport processes in a liquid-filled rectangular enclosure of finite size (Tou *et al*., 1999; Tou and Zhang 2003). The interactions of flows tangential and normal to the heater surfaces in an inclined enclosure were found to cause a slight oscillation in Nusselt number. Inclination was found to have little effects on the average heat transfer characteristics. In case of configurations close to the conduction case with heaters on top, a sharp decrease in Nusselt number was found. Correlations for the row average Nusselt number versus Rayleigh number at various inclination angles were presented.

Steady natural convection induced by multiple discrete heat sources (DHSs) in two-dimensional horizontal enclosures was numerically investigated Deng *et al*., 2002). Four different calculation cases were detailed analyzed, and main attention was focused on the effects of the Rayleigh number, the thermal strength and the separation distance on the interaction between DHSs. Computational results demonstrated that, the combined temperature scale method and the unified heat transfer characteristics analysis were convenient. In addition, it was proved to be efficient in evaluating the complex interaction between DHSs and its effects on the fluid flow and heat transfer structures in horizontal natural convection enclosures.

A numerical study was performed to investigate the effect of aspect ratio on the natural convection of a fluid contained in a rectangular cavity with 50% active side walls (Nithyadevi *et al*., 2007). The active part of the left side wall was at a higher temperature than that of the right side wall. The top and bottom of the cavity and inactive part of the side walls were thermally insulated. Nine different relative positions of the active zones were considered. The heat transfer rate was high for the bottom–top thermally active location while the heat transfer rate was proved to be poor in the top–bottom thermally active location. The heat transfer rate was found to increase with an increase in the aspect ratio.

Laminar natural convection heat transfer inside fluid-filled, tilted square cavities cooled at one side and partially heated at the opposite side was studied numerically (Corcione and Habib, 2010). Simulations were performed for a complete range of heater sizes and locations, Rayleigh numbers based on the side of the cavity from 1.0×10^3 to 1.0×10^7, Prandtl numbers from 0.7 to 700, and tilting angles of the enclosure from $+75^o$ to -75^o. Generally, the heat transfer rate was increased with the increase of the Rayleigh number, Prandtl number and the heater size. In addition, for negative inclinations of the enclosure the amount of heat exchange was decreased with the increase of tilting angle.

Combined convection in an open channel with a square enclosure which has a partially or fully heated on left side to simulate assisting flow was carried out numerically using finite element method (Rahman *et al*., 2013). The left side of the enclosure was heated fully or partially with an isothermal heater. Inlet temperature of the fluid was colder than that of heater. Thus, two cases were tested as fully heated side and partially heated side. Effects of magnetic field were tested on flow and temperature field inside the channel. It was observed that length of heater became insignificant on flow field for higher values of Hartmann number. On the contrary, higher heat transfer was formed for partial heater at the higher values of Rayleigh number.

Natural convection in a partially heated enclosure was investigated in order to identify the optimum location of the active wall for better heat transfer, in consideration with entropy generation (Mahapatra *et al*., 2015). The effect of active wall positions on heat transfer and entropy generation was studied exhaustively considering six different configurations with enclosure aspect ratios 1.5, 2.0 and 4.0. The thermal mixing and temperature uniformity were also analyzed to find the suitability of present geometry and condition in other relevant applications. From the numerically simulated results, different sets of active wall locations were identified for better heat transfer, thermal mixing and temperature uniformity for Rayleigh number from 1.0×10^3 to 1.0×10^6 and Prandtl number of 0.71.

Secondly, the mass and energy transfer through vents in enclosures by natural ventilation has significant impact on the inner air quality. The existing works available in literatures (Sefcik *et al*., 1991; Nada and Moawed, 2004; El Alami *et al*., 2005; Mahmud and Pop, 2006; Radhakrishnan *et al*., 2010; Liu *et al*., 2011; Harish and Venkatasubbaiah, 2013) considering enclosures with open sides or natural vented openings were received relatively few attentions probably due to the complexity of computations with the open sides.

Natural convection in vertically-vented enclosures is investigated theoretically (Sefcik *et al*., 1991). A vertically vented enclosure is one in which the buoyancy-driven flow and heat transfer were restricted by vents in the top and bottom bounding walls of the enclosure. The results revealed that, strongly non-uniform local heat transfer along the isothermal wall was found as a result of the blockage at the inlet. A local maximum and minimum in heat transfer were occurred in the lower half of the enclosure. The predictions for the flow field revealed that, the heat transfer extremes are attributed to a recirculation zone near the inlet gap and primary flow attachment along the heated wall.

Free convection from a tilted rectangular enclosure heated at the bottom wall and vented by uniform slots opening at different walls of the enclosure was experimentally investigated (Nada and Moawed, 2004). The experiments were carried out to study the effects of venting arrangement, opening ratio and enclosure's tilt angle on the passive cooling of the enclosure. Three different venting arrangements of the air from the enclosure were studied. The results showed that, the Nusselt number is decreased with the increase of tilt angle of the enclosure considering top vent. For side-venting and side and top-venting arrangements, the Nusselt number is increased as the tilt angle increased in the range (0^o, 90^o), then it decreased with the increase of the tilt angle. Correlations were developed for the three venting arrangements to predict the average Nusselt number of the enclosure in terms of the opening ratio and the enclosure tilt angle.

A study of natural convection from a two dimensional horizontal channel with rectangular heated blocks was performed numerically (El Alami *et al*., 2005). The governing equations were solved using a control volume method, and the SIMPLEC algorithm was used for treatment of the pressure-velocity coupling. Special emphasis was given to detail the effect of the blocks spacing (gap) on the heat transfer and the mass flow rate generated by the natural convection. Rayleigh number, Prandtl number, opening width, blocks gap and the blocks height were considered as problem parameters. The flow structure and the heat transfer were found to depend significantly on the control parameters.

Steady mixed convection flow in a vented enclosure with an isothermal vertical wall and filled with a fluid-saturated porous medium was investigated numerically (Mahmud and Pop, 2006). The forced flow conditions were imposed by providing an inlet at the bottom surface and a vent at the top, facing the inlet. The nature and the basic characteristics of the mixed aiding as well as mixed opposing flows that arise were investigated using the Darcy law model. Rayleigh number, Peclet number and the width of the inlet as a fraction of the height of the square enclosure were considered as governing parameters. These parameters were varied over wide ranges and their effect on the heat transfer characteristics was studied in detail. The variation of the problem parameters were found transform the flow pattern from a unicellular flow to a multicellular flow, especially, for small values of Peclet number.

A study of fluid flow and heat transfer in an enclosure was performed experimentally and numerically where, multiple heaters are arranged in a staggered fashion (Radhakrishnan *et al*., 2010). Experiments were carried out for different values of Reynolds numbers and Grashof numbers. Numerical simulations were carried out for two-dimensional, steady and incompressible turbulent flow. The results of the numerical study were compared with the experimental results. An insight into the power management among the heaters were presented using the temperature distribution, so that the ''coolest'' heater can be loaded most to maximize the total heat dissipation. Two methods were used to achieve the target temperature for all heaters, namely (i) trial and error method and (ii) the response surface method. The method of response surface was found to be effective in optimizing the total heat transfer for a given target temperature.

Simultaneous transport of heat and moisture by conjugate natural convection in a partial enclosure with a solid wall was investigated numerically (Liu *et al*., 2011). The fluid, heat and moisture transports through the cavity and solid wall were analyzed using the streamlines and isotherms. The heat and mass transfer potentials were also explained by the variations of overall Nusselt and Sherwood numbers. It was shown that, the heat transfer potential, mass transfer potential, and volume flow rate can be promoted or inhibited, depending strongly on the wall materials and size, thermal and moisture Rayleigh numbers.

The buoyancy-induced turbulent flow generated by a heat source in a square enclosure with single and multiple ceiling vents was studied numerically (Harish and Venkatasubbaiah, 2013). A two-dimensional, turbulent natural convection flow was investigated in stream function and vorticity formulation approach. Results are reported for different Grashof numbers varied from 1.0×10^8 to 1.0×10^{10}. The effects of heat source location, vent location and multiple vents on flow characteristics in enclosure were presented. Significant change was found in the flow behavior by varying the location of heat source and vent for fixed Grashof number. The volume flow rates through the two ceiling vents were showed a significant variation depending on the location of vent.

In the present study, a three dimensional steady laminar natural convection in discretely heated small rectangular enclosures is investigated theoretically. A discrete heat source mounted on the substrate at the bottom wall is used with top opening vent. Both conduction in the component and substrate are included. Three types of heat source are studied, concentrated heat source, line heat source and uniformly distributed heat source. The Rayleigh number, vent aspect ratio, enclosure aspect ratio and enclosure walls temperature are considered as problem parameters. Solutions are obtained for Rayleigh number ranging from 1.0×10^4 to 1.0×10^6, enclosure aspect ratios ranging from 0.1 to 1.0; vent aspect ratio ranging from 0.0 to 0.1 and Prandtl number of 0.7. The flow and thermal pattern within the enclosure are presented. Consequently, the local and overall heat transfer in terms of Nusselt number and the surface temperatures are presented to illustrate the vent effects.

Theoretical Model

A mathematical model is proposed to describe the natural convection heat transfer from a hot horizontal heat source. A three-dimensional enclosure confined by four isothermal walls at a uniform temperature of T_o is considered. The enclosure base length and width are L_1, L_2 while L_3 is the enclosure height. The heat source, in *x-y* plane, is buried, horizontally, in an enclosure with vent at the upper wall. The vent is set to be square shape with side length equal to *s*. The physical description of the problem and the coordinate system considered in the present model are shown in Figure 1.

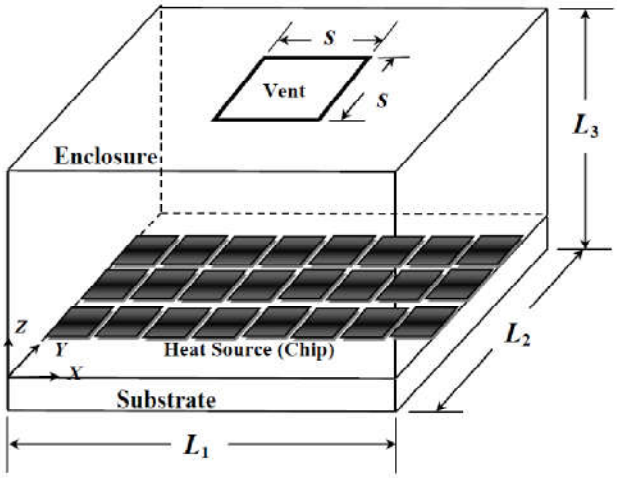

Figure 1. Schematic diagram of the examined enclosure and the shape of vent

Accordingly, the problem can be, fairly, analyzed as a three dimensional laminar flow with free convective at constant physical properties. Cartesian coordinate system (*x, y, z*) is used to express the flow governing equations. The governing equations are written as follow:

$$\frac{\partial u}{\partial x}+\frac{\partial v}{\partial y}+\frac{\partial w}{\partial z}=0 \tag{1}$$

$$w\frac{\partial w}{\partial z}+u\frac{\partial w}{\partial x}+v\frac{\partial w}{\partial y}=-\frac{1}{\rho}\frac{\partial p}{\partial z}+\frac{\mu}{\rho}\left(\frac{\partial^2 w}{\partial x^2}+\frac{\partial^2 w}{\partial y^2}+\frac{\partial^2 w}{\partial z^2}\right)+g\beta(T-T_o) \tag{2}$$

$$w\frac{\partial u}{\partial z}+u\frac{\partial u}{\partial x}+v\frac{\partial u}{\partial y}=-\frac{1}{\rho}\frac{\partial p}{\partial x}+\frac{\mu}{\rho}\left(\frac{\partial^2 u}{\partial x^2}+\frac{\partial^2 u}{\partial y^2}+\frac{\partial^2 u}{\partial z^2}\right) \tag{3}$$

$$w\frac{\partial v}{\partial z}+u\frac{\partial v}{\partial x}+v\frac{\partial v}{\partial y}=-\frac{1}{\rho}\frac{\partial p}{\partial y}+\frac{\mu}{\rho}\left(\frac{\partial^2 v}{\partial x^2}+\frac{\partial^2 v}{\partial y^2}+\frac{\partial^2 v}{\partial z^2}\right) \tag{4}$$

$$\rho C_p\left(w\frac{\partial T}{\partial z}+u\frac{\partial T}{\partial x}+v\frac{\partial T}{\partial y}\right)=k\left(\frac{\partial^2 T}{\partial x^2}+\frac{\partial^2 T}{\partial y^2}+\frac{\partial^2 T}{\partial z^2}\right)+H \tag{5}$$

Equation (1) is considered as the continuity equation of the three dimensional flow with the velocity components in *x*-, *y*- and z-directions of *u*, *v and w* respectively. Equations (2)-(4) are considered as the momentum equations in both the *x*-, *y*- and *z*-directions respectively. Where, ρ, p, μ and β are denoted to density, pressure, dynamic viscosity and the coefficient of thermal expansion respectively. The temperature of the fluid and the heat source per unit time and unit volume are denoted by T and H as shown in energy equation (5). Where, the thermal conductivity and specific heat of the fluid are denoted by k and C_p respectively. Considering the energy equation (5), the heat source is defined according to the following equation (Myrum, 1990; Mousa, 2006):

$$H=10.2\times x+4.1\times y+4 \tag{6}$$

The governing equations (1)-(5) must satisfy the following boundary conditions:

$$\begin{aligned}
&At\ z=0.0,\ \ 0.0\le y\le L_2,\ 0.0\le x\le L_1:\ \ u=v=w=0.0,\frac{\partial T}{\partial y}=-\frac{q''}{k},p=0.0\\
&At\ z=L_3,\ 0.0\le y\le \frac{L_2-s}{2},\ 0.0\le x\le \frac{L_1-s}{2}:\ \ u=v=w=0.0,T=T_o,\frac{\partial p}{\partial z}=0.0\\
&At\ z=L_3,\ \frac{L_2+s}{2}\le y\le L_2,\ \frac{L_1+s}{2}\le x\le L_1:\ \ u=v=w=0.0,T=T_o,\frac{\partial p}{\partial z}=0.0\\
&At\ z=L_3,\ \frac{L_2-s}{2}\le y\le \frac{L_2+s}{2},\ \frac{L_1-s}{2}\le x\le \frac{L_1+d}{2}:\ \frac{\partial u}{\partial y}=\frac{\partial v}{\partial y}=w=0.0,\frac{\partial T}{\partial y}=0.0,\frac{\partial p}{\partial z}=0\\
&At\ x=0,\ \ 0.0\le y\le L_2,\ 0.0\le z\le L_3:\ \ u=v=w=0.0,T=T_{w23}\\
&At\ x=L_1,\ \ 0.0\le y\le L_2,\ 0.0\le z\le L_3:\ u=v=w=0.0,T=T_{w23}\\
&At\ y=0,\ \ 0.0\le x\le L_1,\ 0.0\le z\le L_3:\ \ u=v=w=0.0,T=T_{w13}\\
&At\ y=L_2,\ \ 0.0\le x\le L_1,\ 0.0\le z\le L_3:\ \ u=v=w=0.0,T=T_{w13}
\end{aligned} \tag{7}$$

Referring to boundary condition equation (7), the value of dimension, *s*, is set to zero in case of closed enclosure. Solving the governing Equations (1)-(5) with the aid of boundary conditions (6), one can obtain the temperature and velocity distribution throughout the flow field. Consequently, the value of local heat transfer coefficient, the local Nusselt number and the average Nusselt number are calculated according to the following relations:

$$h=\frac{q''}{(T_{max}-T_0)},\ Nu_L=\frac{h\,L_1}{k}\ \text{and}\ Nu_{av}=\frac{1}{L_1}\int Nu_L\,dL \tag{8}$$

Where q'' and T_{max} are the heat flux and the maximum temperature respectively. The characteristic length, L_1, is assumed equal to the side length in case of a square enclosure and the base length in case of a rectangular enclosure. To put the governing equations and their boundary conditions in a dimensionless form, the following dimensionless independent and dependent variables are introduced as follow:

$$\begin{aligned}
&X=\frac{x}{L_1},Y=\frac{y}{L_1},Z=\frac{z}{L_1},U=u\frac{L_1}{\nu},V=v\frac{L_1}{\nu},\\
&W=w\frac{L_1}{\nu},\mathrm{P}=\frac{p}{\rho}\times\left(\frac{L_1}{\nu}\right)^2\ \text{and}\\
&\theta=\frac{8k}{H{L_1}^2}(T-T_0)
\end{aligned} \tag{9}$$

The values of *U*, *V* and *W* are considered as the dimensionless velocity component in *X*-, *Y*-and *Z*- direction respectively. Where, ν and θ are the kinematics viscosity and the dimensionless temperature respectively. Substituting the

dimensionless variables into Equations (1)-(5), the dimensionless forms of the governing equations are obtained as follow:

$$\frac{\partial U}{\partial X}+\frac{\partial V}{\partial Y}+\frac{\partial W}{\partial Z}=0 \tag{10}$$

$$\frac{\partial U}{\partial X}+\frac{\partial V}{\partial Y}+\frac{\partial W}{\partial Z}=0 \tag{11}$$

$$U\frac{\partial U}{\partial X}+V\frac{\partial U}{\partial Y}+W\frac{\partial U}{\partial Z}-\nabla^2 U=-\frac{\partial P}{\partial X} \tag{12}$$

$$U\frac{\partial V}{\partial X}+V\frac{\partial V}{\partial Y}+W\frac{\partial V}{\partial Y}-\nabla^2 V=-\frac{\partial P}{\partial Y} \tag{13}$$

$$U\frac{\partial W}{\partial X}+V\frac{\partial W}{\partial Y}+W\frac{\partial W}{\partial Z}-\nabla^2 W=-\frac{\partial P}{\partial Z}+8\,\frac{Ra}{\mathrm{Pr}}.\theta \tag{14}$$

$$U\frac{\partial \theta}{\partial X}+V\frac{\partial \theta}{\partial Y}+W\frac{\partial \theta}{\partial Z}-\frac{1}{\mathrm{Pr}}\nabla^2\theta=\frac{8}{\mathrm{Pr}} \tag{15}$$

Where, Pr and *Ra* are Prandtl and Rayleigh numbers respectively, which are defined according to the following equations:

$$\mathrm{Pr}=\frac{\nu}{\alpha}\ \text{and}\ Ra=\frac{g.\beta}{\alpha.\nu}\left(\frac{L_1}{2}\right)^3\frac{H\,L_1^{\,2}}{8k} \tag{16}$$

The dimensionless form of governing equations (8)-(15) must satisfy the following boundary conditions;

$$\begin{aligned}
&At\ Z=0.0,\ \ 0.0\le Y\le\frac{L_2}{L_1},\ 0.0\le X\le 1: U=V=W=0.0,\frac{\partial\theta}{\partial Y}=1,P=0.0\\
&At\ Z=\frac{L_3}{L_1},\ 0.0\le Y\le\frac{L_2-s}{2\cdot L_1},\ 0.0\le X\le\frac{L_1-s}{2L_1}: U=V=W=0.0,\theta=0.0,\frac{\partial P}{\partial Z}=0.0\\
&At\ Z=\frac{L_3}{L_1},\ \frac{L_2+s}{2\cdot L_1}\le Y\le\frac{L_2}{L_1},\ \frac{L_1+s}{2L_1}\le X\le 1: U=V=W=0.0,\theta=0.0,\frac{\partial P}{\partial Z}=0.0\\
&At\ Z=\frac{L_3}{L_1},\ \frac{L_2-s}{2\cdot L_1}\le Y\le\frac{L_2+d}{2\cdot L_1},\ \frac{L_1-s}{2L_1}\le X\le\frac{L_1+s}{2L_1}: \frac{\partial U}{\partial Y}=\frac{\partial V}{\partial Y}=W=0,\frac{\partial\theta}{\partial Y}=0,\frac{\partial P}{\partial Z}=0\\
&At\ \ X=0,\ \ 0.0\le Y\le\frac{L_2}{L_1},\ 0.0\le Z\le\frac{L_3}{L_1}: U=V=W=0.0,\theta=\theta_{w23}\\
&At\ \ X=1,\ \ 0.0\le Y\le\frac{L_2}{L_1},\ 0.0\le Z\le\frac{L_3}{L_1}: U=V=W=0.0,\theta=\theta_{w23}\\
&At\ \ Y=0,\ \ 0.0\le X\le 1,\ 0.0\le Z\le\frac{L_3}{L_1}: U=V=W=0.0,\theta=\theta_{w13}\\
&At\ \ Y=\frac{L_2}{L_1},\ \ 0.0\le X\le 1,\ 0.0\le Z\le\frac{L_3}{L_1}: U=V=W=0.0,\theta=\theta_{w13}
\end{aligned} \tag{17}$$

The dimensionless form of governing equations (8)-(15) with their boundary conditions equation **Error! Reference source not found.** are applied for both a uniformly distributed and concentrated heat source in the case of equal wall-temperature. In the case of different wall-temperature, using the same governing equations, the dimensionless temperature of the left *x-z* plane in enclosure is set to be not equal to zero. Considering the dimensionless energy equation **Error! Reference source not found.**, the right-hand side of the equation, (8/Pr), represented the heat source-term. The heat-source term is appeared at all nodes in the mesh considering the case of uniformly distributed heat source. For the concentrated heat source, the heat source parameter is appeared only at the nodes where, the heat source is existed on it and it equal to zero at all the other nodes. Similarly, the heat source parameter is appeared only at the nodes on specific line where, the heat source is existed on it and it equal to zero at all the other nodes considering line heat source.

To solve the dimensionless form of governing equations (8)-(15), the derivatives of the variables are replaced by the corresponding approximate finite divided differences (21). The first and second derivatives with respect to *X, Y* and *Z* are approximated by centered finite divided difference technique. According to the mentioned technique, the momentum and energy equations are converted to four sets of algebraic equations. These systems of algebraic equations are solved using the gauss-elimination method. An iterative solution procedure is employed to achieve convergence of the solution of the problem.

A 3-D, non-uniform and staggered grid is used to discretize the physical domain. Grid independence is established by examining the heat transfer from the surfaces of the heat sources. Test runs are performed on a series of non-uniform grids to determine the grid size effects. Since a wide range of modified Rayleigh number is considered, the tests are conducted for three modified Rayleigh numbers at 1.0×10^4, 1.0×10^5 and 1.0×10^6. The maximum difference in the row-averaged Nusselt number between grid (37×31×61) and grid (95×31×91) is 3.5% for row 5 at $Ra=1.0\times10^5$. The difference in the row-averaged Nusselt number between grid (51×31×61) and grid (95×31×91) is less than 0.35%. Thus, the former grid (51×31×91) is used in subsequent computations. A computer program in FORTRAN is developed to perform the numerical solution. The dimensionless velocity and temperature at different position are obtained. Consequently, local Nusselt number and average Nusselt number are derived with the aid of their definitions.

RESULTS AND DISCUSSION

The present theoretical model is used to study the effect of Rayleigh number, vent aspect ratio, *VAR*, enclosure aspect ratio, *AR*, and enclosure walls temperature on the flow and isotherm patterns. Three types of heat source are studied, concentrated heat source, line heat source and uniformly distributed heat source. Accordingly, local and average Nusselt numbers are obtained. Solutions are obtained for Rayleigh number ranging from 1.0×10^4 to 1.0×10^6, enclosure aspect ratios ranging from 0.1 to 1.0, vent aspect ratios ranging from 0.0 (closed) to 0.01 and Prandtl number of 0.7.

Validity of the present model

In order to check the validity of the present proposed model, a comparison is made between the present numerical results and the corresponding previous theoretical and experimental results at the same conditions. A comparison is made between the present numerical results and the corresponding previous theoretical results (Tou and Zhang,2003; Mousa, 2006) as shown in Table (1) considering the calculated maximum temperature.

Considering uniformly distributed heat source, the values of Rayleigh number, Prandtl number and aspect ratio, AR, are found to be 1.0×10^5, 0.7 and 1.0 respectively. A fairly good agreement is found between results.

Table 1. Comparison between the present results and previous results (6, 20) for a uniformly distributed heat source at Ra= 1.0×10^5, Pr = 0.70 and AR =1.0 for closed enclosure

Tou and Zhang 2003		Mousa 2006		Present study	
θ_{max}	mesh size	θ_{max}	mesh size	θ_{max}	mesh size
0.259	37 × 31 × 61	0.238	21 × 21 × 21	0.252	37 × 31 × 61
0.264	35 × 31 × 91	0.247	41 × 41 × 41	0.265	35 × 31 × 91
0.265	55 × 31 × 91	0.249	61 × 61 × 61	0.268	51 × 31 × 61

Another check is made by comparing the present numerical average Nusselt number results with the previous experimental results (Myrum, 1990) considering the same working conditions for different values of Rayleigh number and AR=1.0 as shown in Figure 2. A fairly good agreement is found between present and previous results. In general, the average Nusselt number is increased with the increase of Rayleigh number. Considering the present results, the average Nusselt number is found to take higher values for top vented enclosure than for closed enclosure.

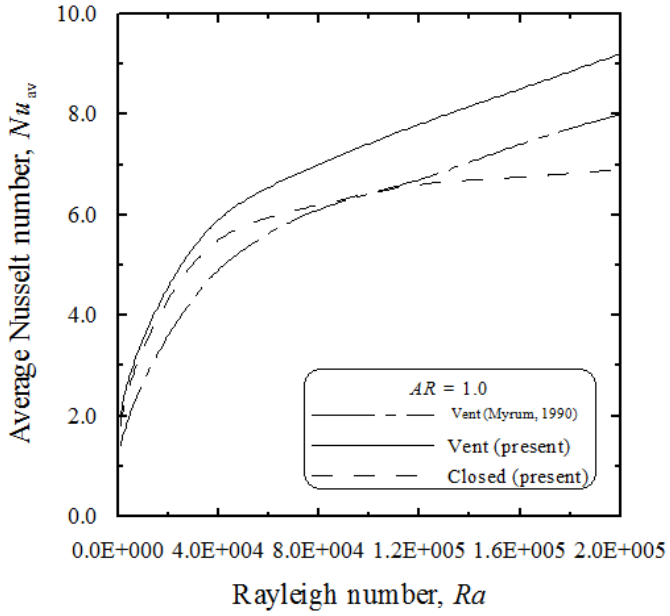

Figure 2. Comparison between present and previous values of the average Nusselt number for different value of Rayleigh number

Streamline and Isotherm Contours

The streamline and isotherm contours in selected plane inside enclosure with aspect ratio of 1.0 and vent aspect ratio of 0.05 for different values of Rayleigh number and at Pr=0.7 is shown in Figure 7. The selected X-Z plane is located at Y=0.2 considering concentrated heat source is shown in figure 3 and Figure 4. The concentrated heat source is set at point (0.5, 0.5, 0.0).

The streamline contours are presented as two counter rotating rolls as shown in Figure 3. The peak-value of stream function is increased with the increase of Rayleigh number. At the values of Rayleigh number equal to 1.0×10^5 and 5.0×10^5, variation is, strongly, noticed in stream function values. The existing of secondary flow adjacent to the top of the enclosure is the suggested reason. As a fact, the heat dissipation from the heat source is concentrated around the heat source. The buoyancy force effect is dominant and the heat is transferred mainly by natural convection. The fluctuation of dimensionless temperature is associated with the occurrence of secondary flow as shown in figure 4. In general, the temperature is increased, rapidly, near the walls at X = 0 and 1.0. On the other hand, the values of dimensionless temperature are decreased with the increase of the Rayleigh number. Anywhere far from the walls, the temperature is found to remain almost constant, specially, for smaller values of Rayleigh number. The effect of vent is noticed near the upper wall, specially, for higher values of Rayleigh number.

The effect of varying the Rayleigh number on the streamline and isotherm contours in enclosure with AR = 1.0, VAR=0.05 and Pr=0.7 considering line heat source is shown in figure 5 and figure 6. The line heat source is existed along the enclosure bottom with coordinate Y= 0.5 and Z=0.0 respectively. Generally, near the heat source, the stream function is decayed while the temperature gradient is increased rapidly. So, the conduction is predominant adjacent to location of the heat source. The streamline contour is observed as two counter-rotating rolls. At Ra >1.0×10^4, the left roll is provided with a relatively higher dynamic momentum; hence it enlarged toward the right side while the right roll relatively attenuated referring to Figure 5.

Two high temperature regions are observed in both left and right sides; and adjacent to the heat source position, specially, at higher values of Rayleigh number as shown in Figure 6. The major of the heat is accumulated at upper of the heat source and decay rapidly near the walls. The position of high temperature region with respect to the enclosure walls is depended on the type of heat source.

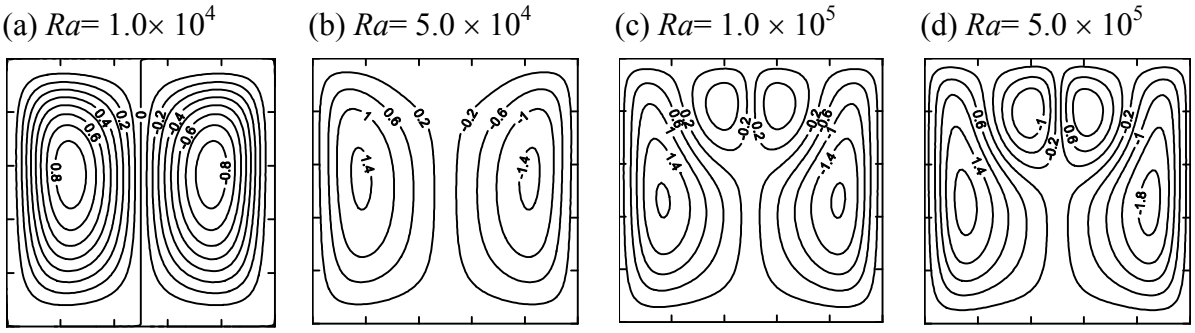

Figure 3. Effect of Rayleigh number on streamline contours at Y=0.2 for AR=1.0, VAR=0.05 and concentrated heat source

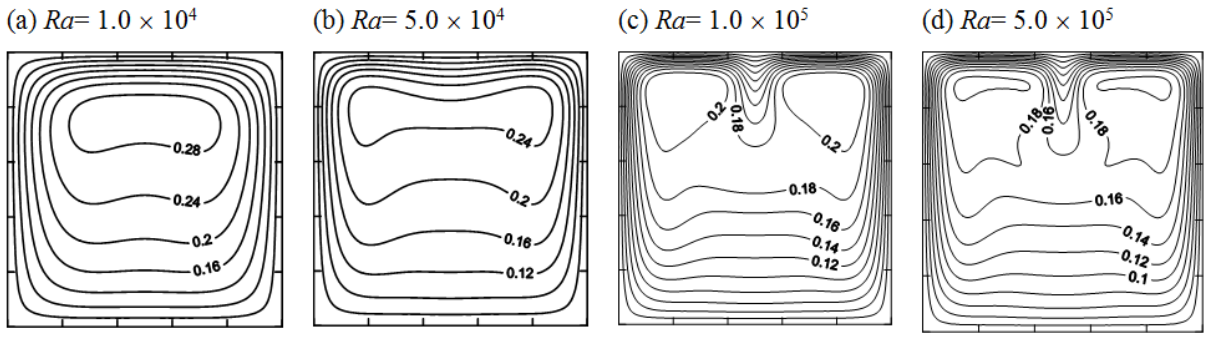

Figure 4. Effect of Rayleigh number on isotherm contours at *Y*=0.2 for *AR*=1.0, *VAR*=0.05 and concentrated heat source

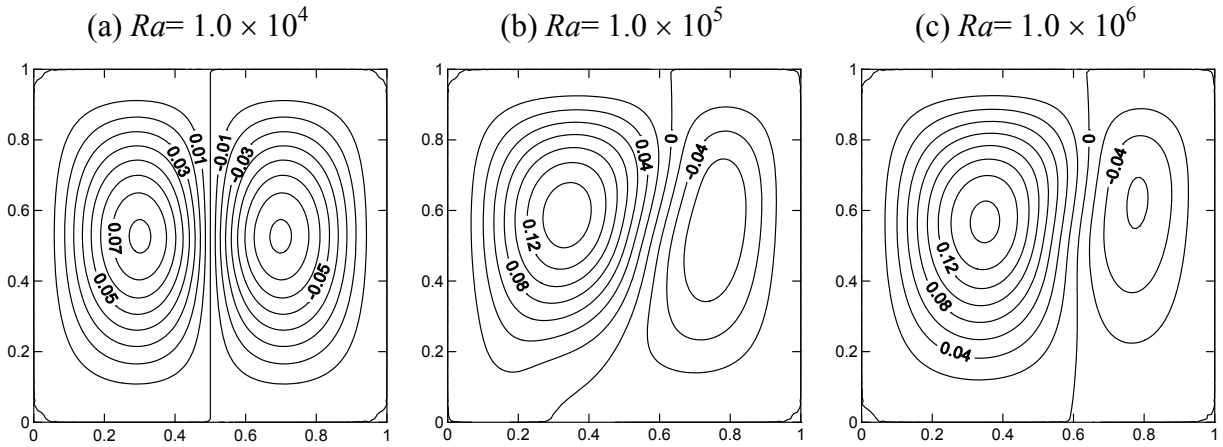

Figure 5. Effect of Rayleigh number on streamline contours at *Y*=0.5 for *AR*=1.0, *VAR*=0.05 and line heat source

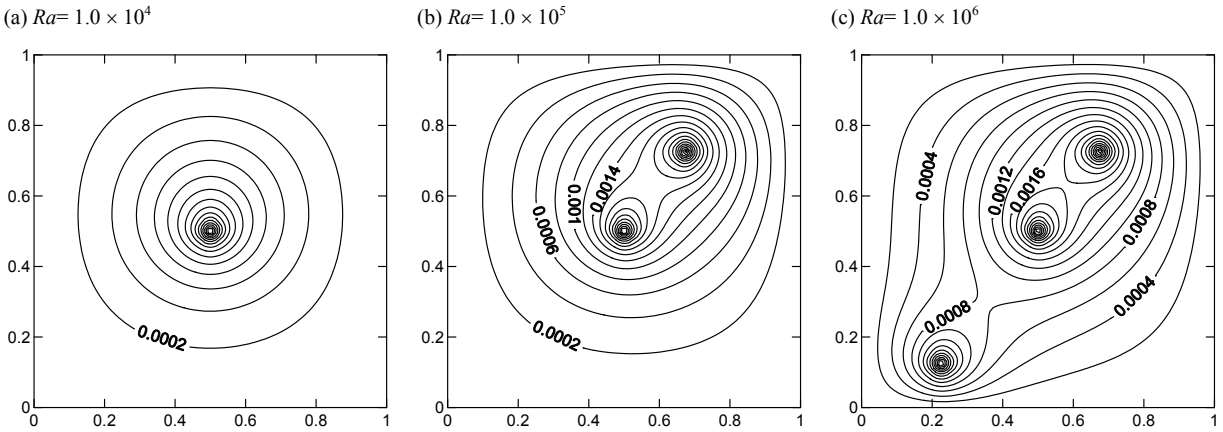

Figure 6. Effect of Rayleigh number on isotherm contours at *Y*=0.5 for *AR*= 1.0, *VAR*=0.05 and line heat source.

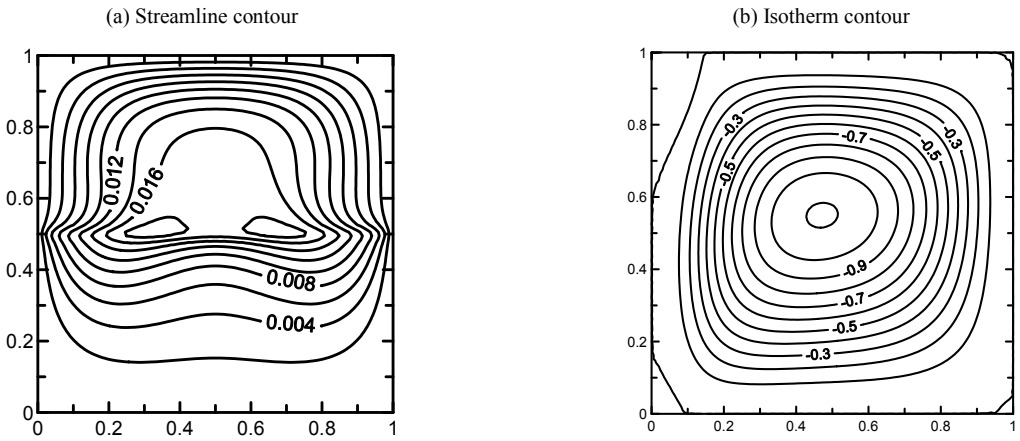

Figure 7. The streamline and isotherm contours in plane parallel to bottom at *Z*=0.2 for *AR*=1.0, *VAR*=0.05, *Ra*=1.0 × 10^5 and line heat source

The streamline and isotherm contours in selected plane inside enclosure with aspect ratio of 1.0 and vent aspect ratio of 0.05 for Rayleigh number equal to 1.0×10^5 and Pr=0.7 is shown in Figure 7. The selected *X*-*Y* plane is located at *Z*=0.2 and parallel to enclosure bottom considering line heat source. The line heat source is existed along the enclosure bottom with coordinate *Y*= 0.5 and *Z*=0.0 respectively.

The value of maximum dimensionless temperature, θ_{max}, and its position for different values of Rayleigh number at *AR* = 1.0 and *VAR*=0.05 is shown in Table 2 considering uniformly distributed heat source. Generally, two positions are observed inside the enclosure for the maximum temperature corresponding to different values of Rayleigh number. The value of maximum dimensionless temperature is decreased with the increase of Rayleigh number. The position of maximum dimensionless temperature is moved continuously toward the top wall with the increase of Rayleigh number.

contours considering the dimensionless wall temperature, θ, equal to -0.2 are shown in Figure 8. The streamline contours is observed as two counter-rotating rolls. The right roll is provided with a relatively higher dynamic momentum; hence it enlarged toward the left side while the left roll relatively attenuated referring to figure 8a. The temperature gradient is increased rapidly adjacent to the left and top walls of the proposed *Y*-*Z* plane referring to figure 8b. Also, the high temperature region is existed exists at vicinity of the top wall.

The streamline contours and isotherm contours considering the dimensionless wall temperature equal to -0.2 are shown in Figure 8. The streamline contour is observed as four-roll structure, two rolls are closed to each other and the other two rolls are separated referring to figure 9a. The two-joined rolls are provided with a relatively higher dynamic momentum, hence they enlarge toward the left side while the two separated rolls attenuate and displace toward the top.

Table 2. Maximum dimensionless temperature and its position for different values of Rayleigh number at *AR* = 1.0 and *VAR*=0.05

Ra	θ_{max}	1st position			2nd position		
		X	*Y*	*Z*	*X*	*Y*	*Z*
1.0×10^4	0.321	0.375	0.271	0.323	0.625	0.271	0.323
5.0×10^4	0.306	0.313	0.271	0.461	0.6974	0.271	,0.461
1.0×10^5	0.294	0.277	0.271	0.551	0.727	0.271	0.551
5.0×10^5	0.276	0.249	0.271	0.593	0.751	0.271	0.593
1.0×10^6	0.258	0.193	0.271	0.637	0.815	0.271	0.637

(a) Streamline contour

(b) Isotherm contour

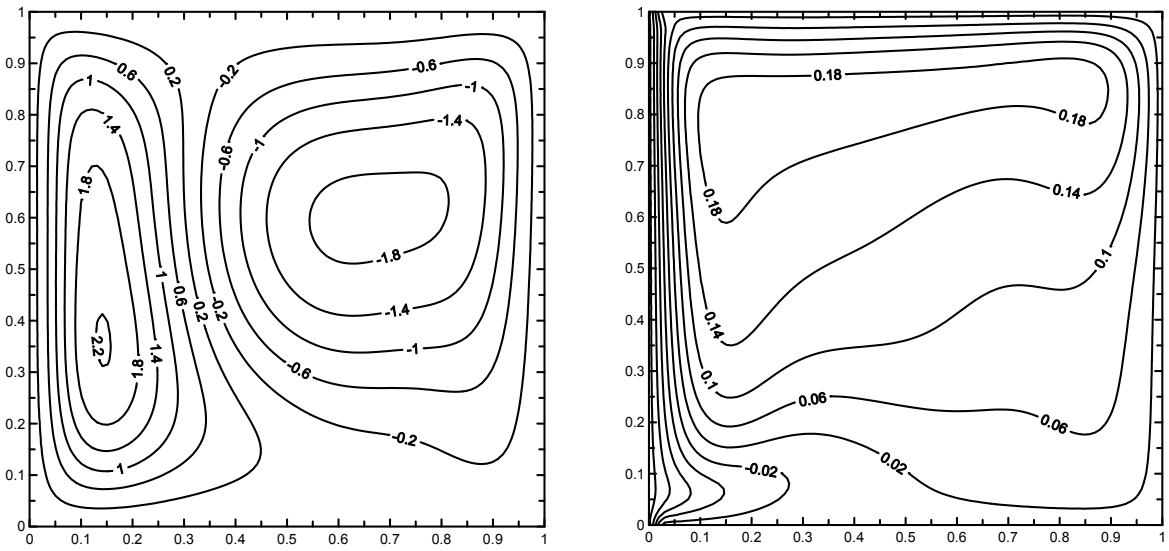

Figure 8. Streamline and isotherm contours in enclosure with θ = -0.2 for *AR*=1.0, *VAR*=0.05 and $Ra=1.0\times10^5$ for uniformly distributed heat source

Enclosure different wall-temperatures

Generally, the temperature distribution and the corresponding flow patterns in the enclosure are affected with the value of wall temperature. To this end, the left *Y*-*Z* plane inside enclosure, at *X*=0.0, is kept at different dimensionless wall temperature while the other sides of the enclosure are maintained at zero dimensionless wall temperature as shown in figure 8 and figure 9 respectively. The enclosure aspect ratio of 1.0 and vent aspect ratio of 0.05 for Rayleigh number equal to 1.0×10^5 and at Pr=0.7 is considered with uniformly distributed heat source. The streamline contours and isotherm

The temperature gradient is increased rapidly adjacent to the left and top walls of the proposed *Y*-*Z* plane. Two high temperature regions are existed at the vicinity of the top wall and near the two side walls referring to Figure 9b.

Heat Transfer Analysis

The local Nusselt number distribution along plane inside enclosure with aspect ratio of 1.0 and vent aspect ratio of 0.05 for Rayleigh number equal to 1.0×10^5 and at Pr=0.7 is shown in Figure 10. The selected Y_2-*Z* plane is located at *X*=0.15 considering concentrated heat source which is existed along the enclosure bottom with coordinate (0.15, 0.5, 0.0).

(a) Streamline contour (b) Isotherm contour

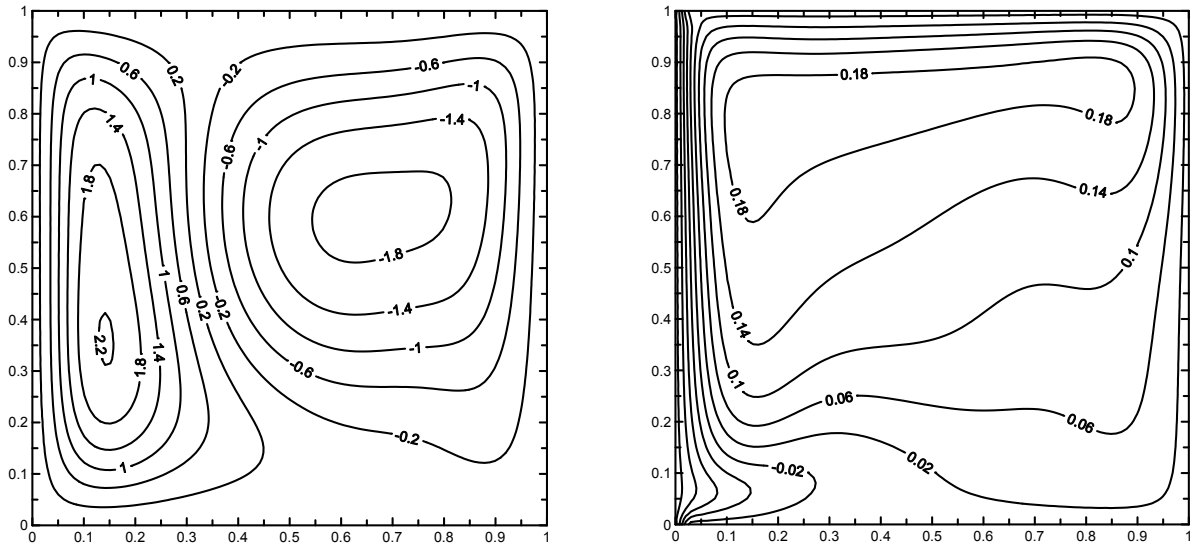

Figure 8. Streamline and isotherm contours in enclosure with θ = -0.2 for *AR*=1.0, *VAR*=0.05 and *Ra*=1.0×10^5 for uniformly distributed heat source

(a) Streamline contour (b) Isotherm contour

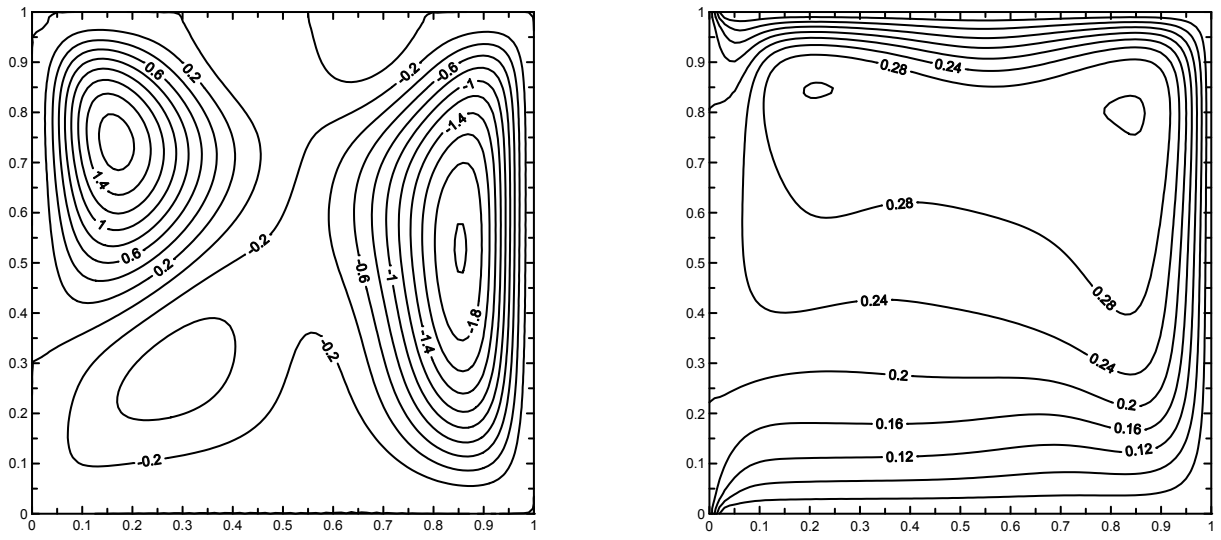

Figure 9. Streamline and isotherm contours in enclosure with θ = 0.2 for *AR*=1.0, *VAR*=0.05 and *Ra*=1.0×10^5 for uniformly distributed heat source

Generally it is noticed that, the local Nusselt number distribution has a peak values near the walls. The highest value of local Nusselt number is noticed at the plane top wall. The local Nusselt number distribution along the plane right wall is found to be similar to plane left wall. The symmetry of plane left wall and plane right wall with respect to line heat source is the suggested reason. Considering the plane bottom wall, no change in the local Nusselt number values are observed around its mid points. The local Nusselt number distribution along top wall of previous plane with aspect ratio of 1.0, Pr=0.7 and Rayleigh number equal to 1.0×10^5 for different values of vent aspect ratio is shown in figure 11. Considering the examined values of *VAR,* the values of local Nusselt number are increased with the decreased of *VAR* values. The trend of local Nusselt number distribution is found be similar in all the examined values of *VAR*.

The effect of varying the aspect ratio on the average Nusselt number for different values of Rayleigh number at vent aspect ratio of 0.05 considering uniformly distributed heat source is shown in Figure 12.a. A number of ten values of aspect ratio are utilized at Pr=0.7. The values of average Nusselt number are increased with the increase of Rayleigh number and aspect ratio. The increase of buoyancy force in addition to large surface is the suggested reason for this increase. The effect of varying the vent aspect ratio on the average Nusselt number for different values of Rayleigh number at aspect ratio of 1.0 and Pr=0.7 considering uniformly distributed heat source is shown in Figure 12.b. A number of eleven values of vent aspect ratio are utilized, in addition to closed vent (*VAR*=0.0) at Pr=0.7. The values of average Nusselt number are increased with the increase of Rayleigh number considering all values of vent aspect ratio. Also, the values of average Nusselt number are increased with the increase of vent aspect ratio for 0.005< *VAR* <0.05. At *VAR*=0.05 a maximum value of average Nusselt

number is obtained considering all values of Rayleigh number. At VAR >0.05, the values of average Nusselt number are decreased with the increase of vent aspect ratio. The random motion of air inside enclosure with larger vent area is the suggested reason for the decrease heat transfer rate.

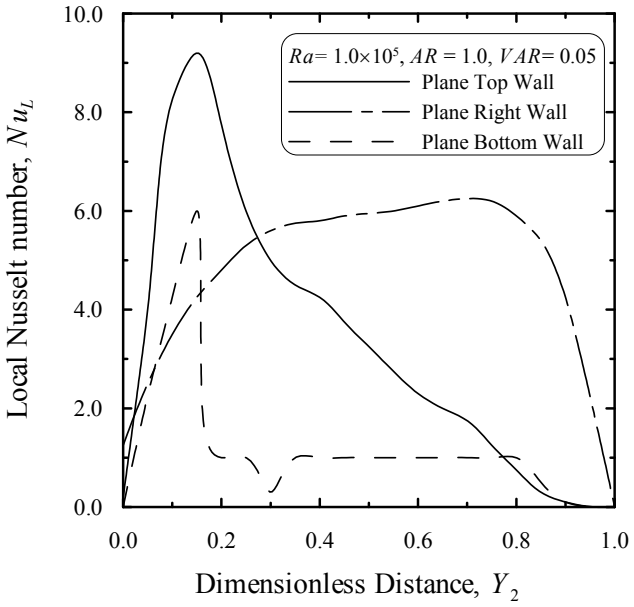

Figure 10. The local Nusselt number distribution along plane walls for AR=1.0, VAR=0.05 and Ra=1 × 10^5

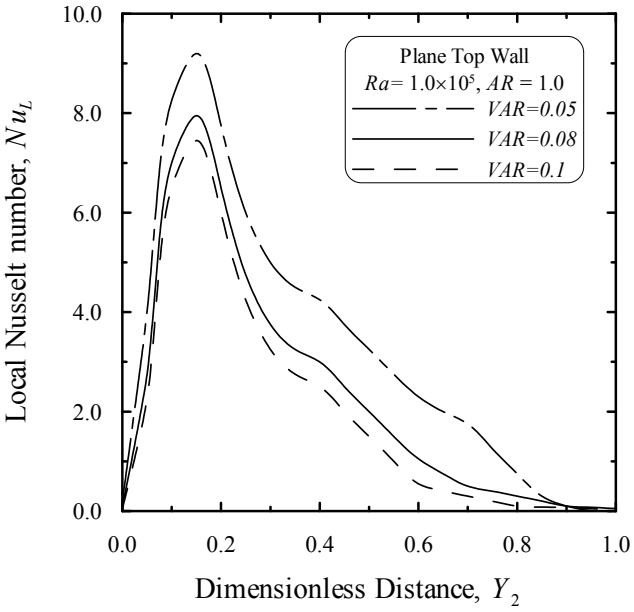

Figure 11. The local Nusselt number distribution along top wall for different values of vent aspect ratio at AR=1.0 and Ra=1 × 10^5

Conclusion

A three-dimensional study of steady laminar natural convection in partially top vented enclosure is investigated numerically. Rayleigh number, vent aspect ratio, enclosure aspect ratio and enclosure walls temperature are considered as problem parameters. A discrete heat source mounted on the substrate at the bottom wall is used to simulate an electronic component.

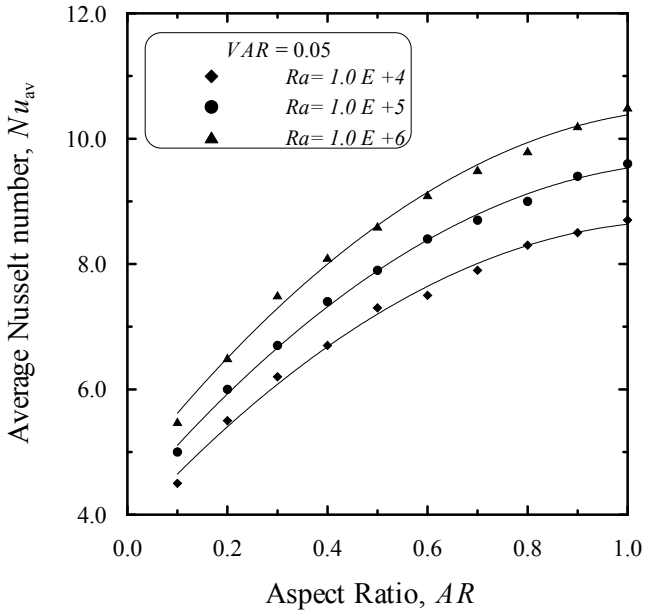

Figure 12.a Relation between average Nusselt number and Aspect ratio for different values of Rayleigh number at VAR= 0.05

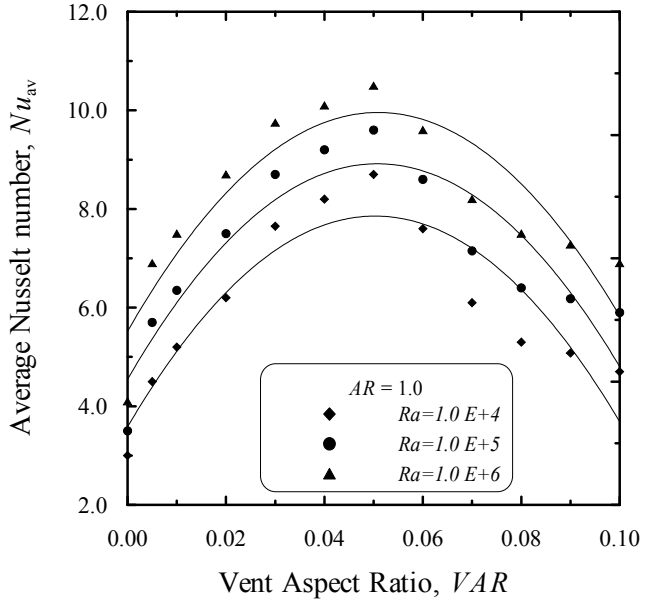

Figure 12.b Relation between average Nusselt number and vent aspect ratio for different values of Rayleigh number at AR=1.0

Three types of heat source are studied, concentrated heat source, line heat source and uniformly distributed heat source. The proposed governing equations are transformed to a set of dimensionless partial differential equations which, is solved with finite difference technique. Solutions are obtained for Rayleigh number ranging from 1.0×10^4 to 1.0×10^6, enclosure aspect ratios ranging from 0.1 to 1.0, vent aspect ratios ranging from 0.0 to 0.01 and Prandtl number 0f 0.7. The resulting flow and temperature patterns are discussed. Accordingly, the values of local and average Nusselt number for different values of problem parameters are obtained. A fairly good agreement is found between the present results and the previous theoretical and experimental studies considering the same operating conditions.

The streamline and isotherm contours are, strongly, depended on problem parameters. Two positions are observed inside the enclosure for the maximum temperature corresponding to different values of Rayleigh number. General, the average Nusselt number is increased with the increase of Rayleigh number and aspect ratio. The average Nusselt number is found to take higher values for top vented enclosure than for closed enclosure. The values of average Nusselt number are increased with the increase of Rayleigh number and aspect ratio. The values of average Nusselt number are increased with the increase of vent aspect ratio for $0.005< VAR <0.05$. At $VAR=0.05$ a maximum value of average Nusselt number is obtained considering all values of Rayleigh number. At $VAR >0.05$, the values of average Nusselt number are decreased with the increase of vent aspect ratio.

REFERENCES

Chadwick M. L., B. W. Webb and H. S. Heaton, "Natural convection from two-dimensional discrete heat sources in a rectangular enclosure," *Int. J. Heat Mass Transfer*, 34 (1991), pp. 1679-1693.

Corcione M. and E. Habib, "Buoyant heat transport in fluids across tilted square cavities discretely heated at one side," *Int. J. Thermal Science*, 49 (2010), pp. 797-808.

Deng Q., G. Tang, Y. Li and M. Ha "Interaction between discrete heat sources in horizontal natural convection enclosures," *Int. J. Heat Mass Transfer*, 45 (2002), pp. 5117-5123.

El Alami M., M. Najam, E. Semma, A. Oubarra and F. Penot, "Electronic components cooling by natural convection in horizontal channel with slots," Energy Conversion & Management 46 (2005), pp. 2762–2772.

Harish R. and K. Venkatasubbaiah, "Numerical simulation of turbulent plume spread in ceiling vented enclosure," *European J. Mechanics B/Fluids,* 42 (2013), pp. 142–158.

Ho C. J. and J. Y. Chang, "A study of natural convection heat transfer in a vertical rectangular enclosure with two-dimensional discrete heating: effect of aspect ratio," *Int. J. Heat Mass Transfer*, 37 (1994), pp. 917-925.

Liu D., F. Zhao and H. Wang, "Passive heat and moisture removal from a natural vented enclosure with a massive wall," *Energy,* 36 (2011), pp. 2867-2882.

Mahapatra P. S., N. K. Manna and K. Ghosh, "Effect of active wall location in a partially heated enclosure," Int. Comm. Heat Mass Transfer 61 (2015), pp. 69-77.

Mahmud S. and I. Pop, "Mixed convection in a square vented enclosure filled with a porous medium," *Int. J. Heat Mass Transfer*, 49 (2006), pp. 2190–2206.

Mousa M. G., "Natural Convection Air cooling of Electronic Components in Partially top vented Enclosures," Mansoura Engineering Journal (MEJ), Faculty of Engineering, Mansoura University 32 (2006), pp. M11-M19.

Myrum T. A., "Natural convection from a heat source in a top-vented enclosure," *ASME J. Heat Transfer*, 112 (1990), pp. 632-639, 1990.

Nada S.A. and M. Moawed, "Free convection in tilted rectangular enclosures heated at the bottom wall and vented by different slots-venting arrangements," *J. Exp. Thermal Fluid Science*, 28 (2004), pp. 853–862.

Nithyadevi N., P. Kandaswamy and J. LeeN, "Natural convection in a rectangular cavity with partially active side walls," *Int. J. Heat Mass Transfer*, 50 (2007), pp. 4688–4697.

Öztop H. F., P. Estellé, W. Yan, K. Al-Salemd, J. Orfi and O. Mahian, "A A brief review of natural convection in enclosures under localized heating with and without nanofluids, " *Int. Comm. Heat Mass Transfer*, 60 (2015), pp. 37-44.

Patankar S., "Numerical Heat Transfer and Fluid Flow," Mc Graw Hill, New York, (1980).

Radhakrishnan T. V., C. Balaji and S. P. Venkateshan, "Optimization of multiple heaters in a vented enclosure – A combined numerical and experimental study," *Int. J. Thermal Science*, 49 (2010), pp. 721-732.

Rahman M. M., H. F. Öztop, R. Saidur, S. Mekhilef and K. Al-Salem, "Finite element solution of MHD mixed convection in a channel with a fully or partially heated cavity," *J. Computers & Fluids*, 79 (2013) , pp. 53–64.

Reay D. A., P. A. Kew and R. J. McGlen, "Heat pipes theory - design and applications," Butterworth-Heinemann, Oxford, pp. 207–225, 2013.

Sefcik D. M., W. Webb and h. S. Heaton, "Analysis of natural convection in vertically-vented enclosures," *Int. J. Heat Mass Transfer,* 34 (1991), pp. 3037-3046.

Tou S. K. W., C. P. Tso and X. Zhang, "3-D numerical analysis of natural convective liquid cooling of a 3×3 heater array in rectangular enclosures," *Int. J. Heat Mass Transfer*, 42 (1999), pp. 3231-3244.

Tou S. K. W.and X. Zhang, "Three-dimensional numerical simulation of natural convection in an inclined liquid-filled enclosure with an array of discrete heaters," *Int. J. Heat Mass Transfer*, 46 (2003), pp. 127-138.

****